

## 1 Supplementary Information

### 1.1 Numerical method

To model the impact events, we use a Smooth Particle Hydrodynamics (SPH) impact code specially written to model geologic materials<sup>16,17,7</sup>. We include the Tillotson equation of state (compare with ref. 30) and a tensile fracture model<sup>16</sup> (with parameters for basalt) in combination with a standard Drucker-Prager yield criterion for rocky materials. Damaged material is modeled using the Coulomb dry-friction law<sup>28</sup>. Parameters used are (see e.g. 28 and 31): coefficient of internal friction (intact material)  $\mu_i = 1.5$ , coefficient of friction (damaged material)  $\mu_d = 0.8$ , cohesion  $Y_0 = 100$  MPa, yield strength  $Y_m = 3.5$  GPa. The block-model approximation of acoustic fluidization<sup>29</sup> is used as it gives a better match to central peak formation. We use an acoustic fluidization viscosity  $\eta = 10^8$  Pa s and an acoustic fluidization decay constant  $\tau = 250$  s in modeling Veneneia, and  $\tau = 650$  s for Rheasilvia; these parameters give a good match to central peak formation.

Self-gravity is computed using a grid-based solver. To avoid numerical rotational instabilities, the scheme suggested by ref. 32 is used in the simulations including rotation.

For the initial target, we use a  $d = 550$  km diameter solid body with a mantle (basalt with a density  $\rho = 2.7$  g/cm<sup>3</sup>) and a 240 km diameter iron core ( $\rho = 7.8$  g/cm<sup>3</sup>). The crust is not explicitly modeled, but we track the dynamical evolution and redistribution of crustal layers during the simulation. We let the target self-gravitate to its hydrostatic equilibrium before the projectile is released. About  $10^6$  SPH particles are used, so the smoothing length  $h \sim 5$  km. To simulate the formation of the older Veneneia basin, we use a spherical projectile of  $d = 64$  km diameter (basalt,  $\rho = 2.7$  g/cm<sup>3</sup>) with an impact velocity of 5.4 km/s and a impact angle of 90° (head-on impact).

For Veneneia we start with a non-rotating undamaged target. The outcome of this simulation is a fully damaged target that is then used as initial condition for a second run, where we study the formation of Rheasilvia on top of Veneneia. To simulate the formation of Rheasilvia we use a  $d = 66$  km projectile impacting head-on with a velocity of 5.4 km/s, offset 40° from the center of the Veneneia. We include pre-impact rotation with period  $P = P_{Vesta} = 5.3$  h on an axis that goes through the center of the Veneneia basin.

The simulations were stopped at  $t = 2 \cdot 10^4$  s after the impact of the projectile. This time corresponds to  $\sim 10$  dynamical times of  $(G\rho)^{-1/2} \sim 2000$  s, and is about equal to Vesta's rotation period ( $P_{Vesta} = 5.3$  h).

## 1.2 Asymmetric ejecta distribution due to rotation

As it was found in a previous study<sup>7</sup>, pre-impact rotation has a large effect on the ejecta fallback distribution. Since we consider a smaller angle between impact direction and rotation axis, this effect is smaller in the work presented here. (Note that here we also look at the combined ejecta from both impacts.) However, we do find some asymmetry resulting from the rotation. As it can be seen in Figs. 3 and S1, there is a region A ( $\sim 0 - 130^\circ$  E,  $0 - 30^\circ$  S) which is covered by ejecta from greater depth than the corresponding region B on the western side of the crater ( $\sim 210 - 340^\circ$  E,  $0 - 30^\circ$  S). The region A corresponds to the region where we expect some pile-up and double-layering of ejecta due to rotation<sup>7</sup>. Interestingly, this region roughly corresponds to the area with the thickest observed ejecta unit (ref. 9, Supplementary Online Material) and with a higher concentration of high-band-ratio material indicating a diogenite rich region (ref. 13, Figure 1, and page 703). Therefore, pre-impact rotation might partly explain these observed asymmetries in ejecta distribution and the resulting compositional asymmetry.

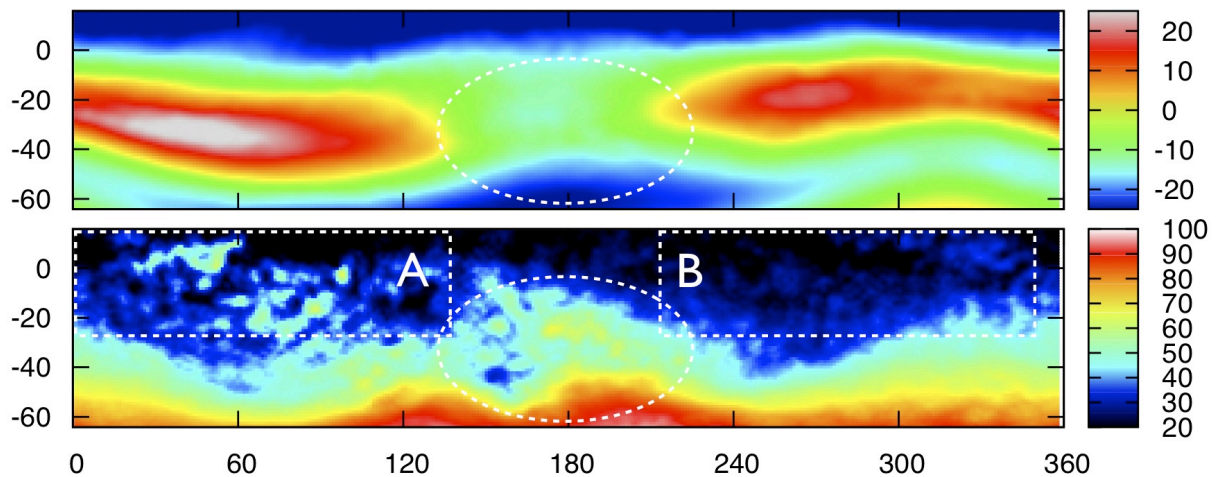


**Figure S1:** Elevation (top) and initial depth of material (bottom) in simple cylindrical projection; the units are in km. Shown is the region from  $16^\circ$ N to  $64^\circ$ S (for comparison to ref. 13). The hemispherical scale dichotomy on Vesta<sup>13</sup> is well reproduced, assuming that diogenite rich material comes from large depths and eucrite rich material from more shallow depth. Rotational effects lead to an additional asymmetry: region A is covered by more ejecta from deeper layers than the ejecta in region B, possibly explaining the observation that the eastern portion of the rim of Rheasilva, between  $\sim 0$  and  $130^\circ$ E, has higher concentrations of high-band-ratio material than the western portion ( $210$  to  $300^\circ$ E) (ref. 13). The dashed ellipse indicates the location of the Veneneia basin.

### 1.3 Escaping ejecta

A fraction of the ejected material reaches velocities greater than the escape speed. We are going to study the implications of these events on the origin of the Vesta family<sup>33</sup> and the HED meteorites (e.g. ref 34). For this, very high resolution simulations focusing on the initial stage of the crater formation are required; at our present model smoothing length of 5 km we cannot yet resolve the largest family members, although a statistical study<sup>6</sup> is feasible.

### 1.4 Accretion of projectile material

A fraction of the material from the projectiles of the two basin forming impacts gets accreted on Vesta. The accreted impactor material could be a potential source for the dark clusters observed by Dawn<sup>14,35</sup>. However, the amount and distribution of accreted impactor material strongly depends on impact conditions (impact velocity and angle) and possibly on the projectile properties; they are subject of a future, more detailed study.

## 2 Supplementary References

30. Melosh, H.J. Impact cratering: A geologic process. Oxford University Press, Oxford, UK. (1989)
31. Collins, G.S., Kenkmann, T., Osinski, G.R., Wünnemann, K. Mid-sized complex crater formation in mixed crystalline-sedimentary targets: Insight from modeling and observation. *MAPS* **43**, 1995 (2008)
32. Speith, R. Improvements of the numerical method smoothed particle hydrodynamics. Habilitation, University of Tuebingen (2006)
33. Binzel, R. P., & Xu, S. Chips off of asteroid 4 Vesta—Evidence for the parent body of basaltic achondrite meteorites, *Science*, **260**, 186 (1993).
34. Consolmagno, G. J. & Drake, M. J. Composition and evolution of the eucrite parent body - Evidence from rare earth elements. *Geochimica et Cosmochimica Acta*, **41**, p. 1271 (1977)
35. Reddy, V., et al. Delivery of Dark Material to Vesta via Carbonaceous Chondritic Impacts. *Icarus* in press (2012)